



ELSEVIER

Journal of Luminescence 60&61 (1994) 281–286

JOURNAL OF  
LUMINESCENCE

### Invited paper

## Reradiation and imaging of diffuse photon density waves using fluorescent inhomogeneities

M.A. O'Leary<sup>a, b</sup>, D.A. Boas<sup>a, b</sup>, B. Chance<sup>b</sup>, A.G. Yodh<sup>a,\*</sup>

<sup>a</sup> Department of Physics, University of Pennsylvania, Philadelphia, PA 19104-6396, USA

<sup>b</sup> Department of Biochemistry and Biophysics, University of Pennsylvania, Philadelphia, PA 19104-6089, USA

### Abstract

Experiments demonstrate the reradiation of diffuse photon density waves in turbid media by an obstacle filled with fluorescent dye. The reradiated energy was also in the form of a diffuse density wave that was readily detected at the red-shifted energy. In this process the inhomogeneity was converted into a source of diffuse photon density waves, and localization of the object can be accomplished by analysis of the reradiated wavefronts. We will discuss these measurements and demonstrate some simple practical devices which are capable of localizing the center of such a fluorescent inhomogeneity.

### 1. Introduction

The transport of visible and near infrared (NIR) photons through dense random media has been the subject of intense recent interest (see e.g. [1]). Important practical aspects of these problems concern the potential uses of diffusing NIR light fields to locate objects within turbid media. To this end, photon migration patterns derived from a variety of probes (see e.g. [2]) have been employed to study the effects of inhomogeneities on optical path lengths in turbid media. In this paper we demonstrate methods whereby fluorescent dyes and amplitude modulated continuous-wave NIR light sources are used to provide imaging information about spatial inhomogeneities within turbid media.

These ideas are potentially useful for studies within the human body, since for example, it is well known that a trace amount of emissive dye (or contrast agent) can equilibrate at spatial inhomogeneities such as breast tumors or infarcted regions of the brain [3].

The paper is organized as follows. We first review the essential aspects of diffuse photon density waves. These propagating disturbances are produced when amplitude modulated light sources are introduced into the dense media. Then we describe simple experiments in model biological media which demonstrate the interaction of diffuse photon density waves with fluorescent inhomogeneities. Finally, we describe more complex methods of detection that provide practical algorithms by which to obtain images. These include spatial encoding by time–amplitude and frequency–gradient techniques, as well as by phased-

\* Corresponding author.

array scanners. We conclude briefly with a description of current issues and future directions.

## 2. Background

Diffuse photon density waves are scalar, overdamped, traveling waves of light energy density,  $U(r, t)$ . They will propagate through any medium in which the transport of light energy density is governed by the diffusion equation. The traveling waves are produced by introducing an amplitude modulated light source into an optically turbid medium [4]. Examples of such media for visible light include dense suspensions of micrometer-size spheres, human tissue, paints, foams, and Intralipid. In essence, the introduction of amplitude modulated light into the turbid medium produces a macroscopic ripple of brightness that is microscopically composed of individual photons undergoing random walks. The disturbances arise formally in any diffusive system that is driven by an oscillating source [4]. The oscillatory part of the solution for an infinite, nonabsorbent, homogenous turbid media in the presence of a point source located at the origin is of the form

$$U(r, t) = (A/Dr)[\exp(-kr)](\exp[i(kr - \omega t)]), \quad (1)$$

where  $A$  is a constant,  $r$  the radial distance from the origin,  $D$  the diffusion coefficient for light in the media,  $\omega$  the source modulation frequency, and  $k = (\omega/2D)^{1/2}$ . Although the wave is very rapidly attenuated, it has a well-defined wavelength, amplitude and phase at all points. Interestingly, this wavelength can be altered by modifying  $D$  or  $\omega$ . When absorption is present, we can derive a similar solution to (1), where the real and imaginary parts of the wave vector  $k$  are different and depend explicitly on the sample absorption length [5]. For simplicity we omit these details from our theoretical discussion, we have, however, included these effects in our analysis of the data.

The macroscopic disturbance obeys a Helmholtz equation, and therefore has many properties that we normally associate with conventional electromagnetic radiation. For example, experiments in this and other laboratories have demonstrated the refraction [6], diffraction [5,7], interference [8,9], and re-emission [7,10] of these waves.

Our experimental apparatus has been previously described [6]. Briefly, a large glass fish tank is filled with a model biological material called Intralipid<sup>1</sup>. Intralipid solution is a turbid, polydisperse suspension of micron size particles. By changing the solution concentration one can vary the light diffusion constant over a wide range. Typically, an amplitude modulated (200 or 50 MHz) laser diode ( $\sim 3$  mW, 780 nm) is fiber-coupled into the medium, and another optical fiber is used to detect diffuse photons as a function of position within the fish tank. Using standard heterodyne techniques, we determine the phase and amplitude of the diffuse photon density wave in the medium. In Fig. 1(a) we show measured constant phase contours of the disturbance produced by our fiber point source located at the origin.

## 3. Re-emission of a diffuse photon density wave from a fluorescent inhomogeneity

The re-emission of a diffuse photon density wave by a fluorescent obstacle was accomplished by filling a spherical glass shell with the absorbing dye Indocyanine green, and then illuminating the sphere with a diffuse photon density wave in the Intralipid solution. The dye was chosen to absorb radiation at the source wavelength of 780 nm, and very soon thereafter reradiate photons at a red-shifted energy, 830 nm. Because the dye had a lifetime of less than 1 ns compared to the 5 ns period of the source, we expect the reradiated energy to be in the form of a diffuse photon density wave at the red-shifted energy. The absorption and emission characteristics of the dye are shown in Fig. 1(b). The quantum efficiency of this dye in water was measured to be  $\sim 1 \times 10^{-2}$ . Our experiments indicate that this efficiency is reduced by more than a factor of 10 in Intralipid solution. The Intralipid solution surrounding the obstacle had a concentration of 0.1%<sup>1</sup> giving a source diffuse photon density wavelength of  $\sim 18$  cm. A point source at the origin generated the incident diffuse photon density wave.

<sup>1</sup> The Intralipid used here can be obtained from Kabi Pharmacia in Clayton, NC. At the 0.1% concentration discussed here, we measure a diffusion coefficient of about  $4.5 \times 10^9$  cm<sup>2</sup> s, a scattering length of 0.7 cm, and an absorption length of 50 cm.

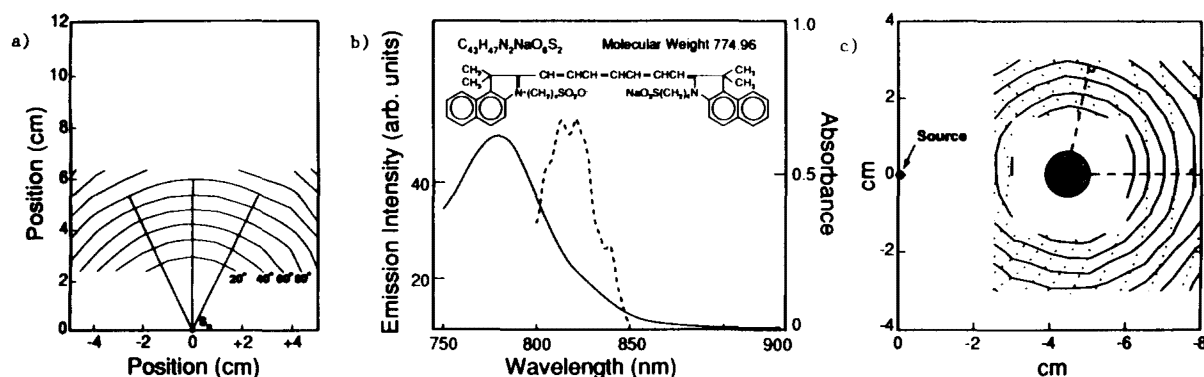


Fig. 1. (a) Constant phase contours shown as a function of position for a homogeneous 0.5% Intralipid solution. The contours are shown on 20° intervals. (b) Indocyanine green absorption (solid line) and emission (broken line) spectra. The inset shows the molecular structure of the dye. (c) Constant amplitude contours at 780 nm (broken lines) and 830 nm (solid lines) clearly exhibiting the reradiated nature of the wave. The amplitude of adjacent contours decreases by a factor of 0.3.

Constant amplitude contours of the incident wave in the presence of the obstacle are shown in Fig. 1(c) (broken lines). Two spectral filters centered on 830 nm (Schott glass filters, RG830) were sufficient to enable us to separate the incident and reradiated waves.

In Fig. 1(c) we exhibit the measured constant amplitude contours of the wave at 830 nm as solid lines, and the measured incident amplitude contours at 780 nm as broken lines, and thereby demonstrate the diffuse photon density wave character of the reradiated waves. We see clearly that reradiated waves originate from within the absorbing obstacle. From the contours we deduce a source origin of ~4.6 cm. The diffuse photon density wavelength at 830 nm was approximately the same as the wave at 780 nm to within a measured error of 35%. This phenomena might be described as a type of fluorescence of a diffuse photon density wave. In the process, the inhomogeneity is converted into a source of secondary diffuse photon density waves.

#### 4. Prototype imaging devices based on fluorescent inhomogeneities

A primary goal of our work is to develop an imaging device and algorithms for use in human subjects. In this section we discuss three imaging devices that we have developed. The ideas are dem-

onstrated in one- or two-dimensional models. We employ sterile Indocyanine green dye for this work.<sup>2</sup> A concentration of 0.4 mg/l was used, less than one tenth of the concentration commonly used in human subjects to test hepatic function.

The first device, shown in Fig. 2 uses multiple sources and a single detector to determine the center of a fluorescent object. We irradiate a fluorescent sphere with multiple sources of diffuse photon density waves, and then measure the amplitude (or phase) of the reradiated light. The partial amplitude resulting solely from source  $i$  is dependent on the  $i$ th source-object separation, the quantum efficiency of the dye, and the object-detector separation according to Eq. (1), i.e.

$$|U_i| \propto \xi \frac{\exp(-k|\vec{r}_i - \vec{r}_0|)}{|\vec{r}_i - \vec{r}_0|} \frac{\exp(-k'|\vec{r}_0 - \vec{r}_d|)}{|\vec{r}_0 - \vec{r}_d|}, \quad (2)$$

where  $\xi$  is the quantum efficiency of the dye,  $\vec{r}_i$  the position of the  $i$ th source,  $\vec{r}_0$  the position of the object center,  $\vec{r}_d$  the detector position, and  $k$  ( $k'$ ) the wave vector magnitude of the diffuse photon density wave at 780 nm (830 nm). The individual sources are separately turned on and off, and the reradiated amplitude for each source-object

<sup>2</sup> Cardio-green is a sterile form of Indocyanine green. We obtained this dye from Hynson, Wescott & Dunning, Inc., Baltimore, MD 21201

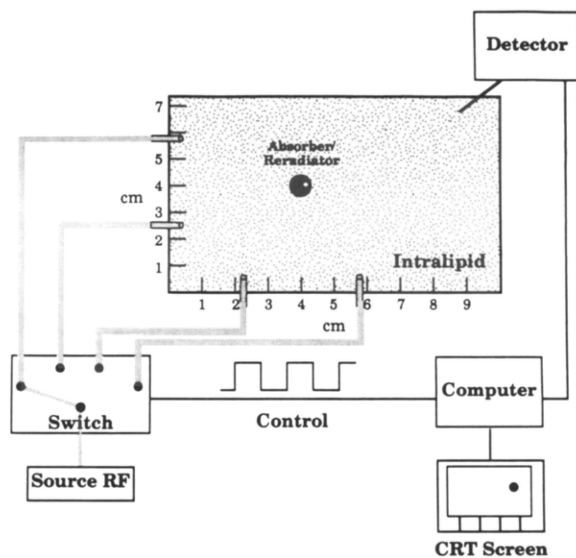


Fig. 2. The time-shared localization device. Four sources are placed at known positions and each source is separately turned on and off. The black circle represents the actual position of the radiator, and the white dot represents the estimated position from the four measured amplitudes.

separation is measured. Since the source positions  $\vec{r}_i$ , and the detector position  $\vec{r}_d$  are known, we estimate the object position by finding the value of  $\vec{r}_0$  that gives the best agreement with the measured ratio  $|U_i|/|U_j|$ . Three sources are necessary to localize the object in two dimensions; we use four to improve the signal to noise of this estimate. The results of such an estimation are shown in Fig. 2. The black circle represent the actual position of the radiator, while the white dot is the computer estimated position. Using four sources we were able to localize the center of this 1 cm sphere to within 0.4 cm. This two-dimensional localization is easily extended to three dimensions.

An attractive alternative to the time-sharing apparatus described above is a frequency encoded device shown in Fig. 3. In this case, each source is modulated by a slightly different modulation frequency,  $f_i$  (i.e.  $f_i = 200.00 + i(0.01)$  MHz) and is kept on at all times. In this way we can associate a modulation power spectrum with each spatial location in the sample. By measuring the power spectrum of the reradiated light as a function of modulation frequency, we can determine the object

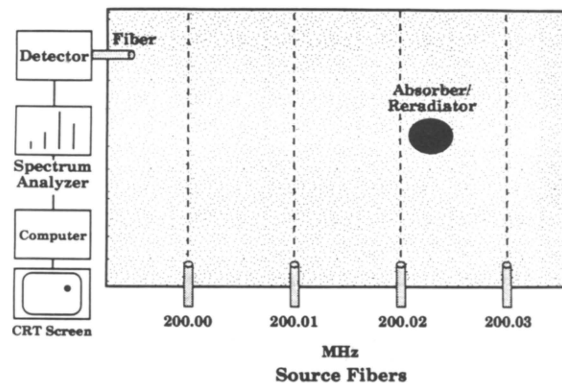


Fig. 3. The frequency-encoded localization device. In this system all four sources are used simultaneously and are modulated at slightly different frequencies. In this way, a modulation frequency spectrum encodes the sample space.

position using essentially the same analysis as above. This scheme is similar in concept to magnetic resonance imaging, in that we convert a frequency spectrum into a spatial location.

A third, qualitatively different imaging device is shown in Fig. 4. It uses a scanning phase-array and a single detector. Specifically, the phased-array [9] consists of two sources 180° out of phase with each other that interfere destructively to produce an amplitude null and a sharp 180° phase shift at points equidistant from the two sources. In two dimensions, the curve that describes this family of points is called the null line (broken line in insets of Fig. 4). If we place a detector on the null line, and then move an *absorbing* object from one side of the line to the other, we find that the object preferentially absorbs light from the nearest source, and therefore distorts the null line. When the absorber is also a radiator, the complimentary effect is seen, that is, the object reradiates more light derived from the closest source. In both measurements the phase of the detected diffuse photon density wave will undergo a 180° shift as the absorber crosses the original, undisturbed null line. These effects are demonstrated in Fig. 4(a). Note that the reradiated light displays a sharper phase transition, and a deeper amplitude null (not shown) than that of the incident light and that the reradiated wave phase exhibits a complimentary change as discussed above.

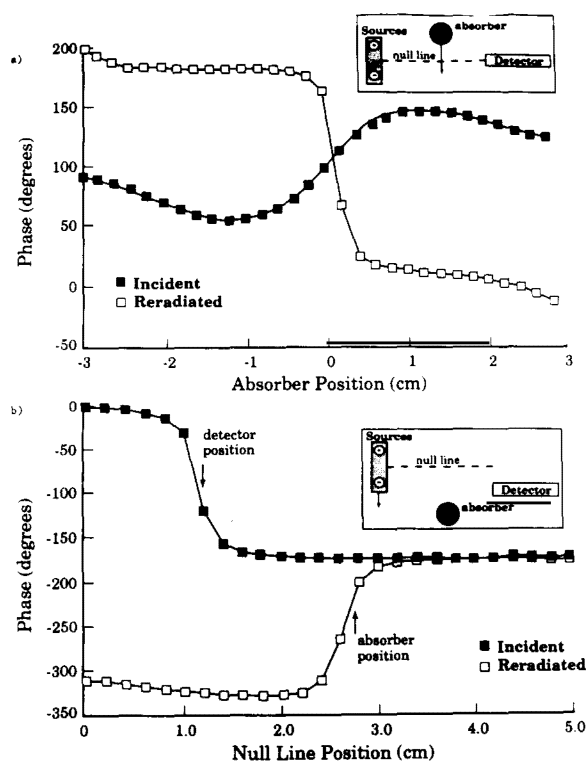


Fig. 4. These experiments were performed with a 50 MHz oscillation frequency in  $\sim 0.4\%$  Intralipid, with a source separation of  $\sim 2.2$  cm. The radiator was located  $\sim 2.0$  cm and the detector  $\sim 4$  cm in front of two anti-phased sources. (a) As shown in the inset, the detector was placed on the null line (broken line) and the radiator was scanned. In the main figure, both the incident and the reradiated light show a  $180^\circ$  phase shift, but the shift is sharper from the reradiated light. (b) Here the source pair and consequently the null line was scanned as shown in the inset. Note that the sharp phase shift from the reradiated (incident) light occurs as the null line crosses the radiator (detector) position.

Interestingly, in the situation depicted in Fig. 4(a), the phase shift of the reradiated light is always the same, independent of detector position. Thus, we can detect essentially the same change by holding the absorber and the detector stationary, and scanning the null line. Scanning of the null line can be achieved by mechanically translating the two sources together. Fig. 4(b) demonstrates this effect for the reradiated light. We detect a sharp phase shift at the location of the radiator as we scan the null line. The phase transition of the inci-

dent light occurs near the position of the detector. If we know the position of the null line as a function of time we achieve a one-dimensional localization of the reradiator. By performing three scans down three perpendicular axes, we can achieve three-dimensional localization.

## 5. Conclusions and future work

We have demonstrated that a fluorescent object illuminated by a diffuse photon density wave becomes a secondary source of diffuse photon density waves at a red-shifted photon energy. We have demonstrated several methods by which the center of the fluorescent object may be localized. Future work must include an improvement in the signal-to-noise ratio which is about 10 for the geometries we used. We are currently looking into better sources and detectors and are hoping to improve the quantum efficiency of the dye. We have also begun work to address the problem of multiple objects/radiators.

## Acknowledgements

We are happy to acknowledge technical assistance from Libo He and Jian Weng. A.G.Y. gratefully acknowledges partial support from the National Science Foundation through the Presidential Young Investigator program and Grant No. DMR-9003687, and from Alfred P. Sloan Foundation. B.C. gratefully acknowledges support from the National Institute of Health Grant Nos. CA50766 and CA60182.

## References

- [1] S. John, *Phys. Today* 44 (5) (1991) 32; S. Feng and P.A. Lee, *Science* 251 (1991) 633; D.J. Durian, D.A. Weitz and D.J. Pine, *Science* 252 (1991) 686 and references therein.
- [2] B.J. Tromberg, L.O. Svaasand, T. Tsay, R.C. Haskell and M.W. Berns, *Future Trends in biomedical applications of lasers*, in: *Proc. Time-Resolved Spectroscopy and Imaging of Tissues*, B. Chance, ed. (SPIE, Bellingham, WA) 143 (1991) and references therein.

- [3] F.W. Flickinger, J.D. Allison, R. Sherry and J.C. Wright, in: Proc. Society of Magnetic Resonance in Medicine 11th Ann. Scientific Meeting, R.N. Bryan, ed., Berlin, Germany, 1992 (Society of Magnetic Resonance in Medicine, San Francisco, 1992) and references therein.
- [4] H.S. Carslaw and J.C. Jaeger, *Conduction of Heat in Solids* (Clarendon Press, Oxford, 1959).
- [5] J. Fishkin and E. Gratton, *J. Opt. Soc. Amer. A* 10 (1993) 127.
- [6] M.A. O'Leary, D.A. Boas, B. Chance and A.G. Yodh, *Phys. Rev. Lett.* 69 (1992) 2658.
- [7] D.A. Boas, M.A. O'Leary, B. Chance and A.G. Yodh, *Phys. Rev. E* 47 (1993) 2999; M.A. O'Leary, D.A. Boas, B. Chance and A.G. Yodh, *SPIE Proc. of the Biomedical Optics Society*, eds. B. Chance and R.R. Alfano, to be published.
- [8] J.M. Schmitt, A. Knüttel and J.R. Knudsen, *J. Opt. Soc. Amer. A* 9 (1992) 1832.
- [9] B. Chance, K. Kang, L. He, J. Weng and E. Sevick, *Proc. Natl. Acad. Sci. USA* 90 (1993) 3423.
- [10] See: A. Knüttel, J.M. Schmitt and J.R. Knutson, *Appl. Opt.* 32 (1993).